Study of a collimation method as a nondestructive diagnostic diagnostic technique by PGNAA for salt distribution in concrete structures at RANS

Yasuo Wakabayashi[1*], *Takao* Hashiguchi[1], *Yuichi* Yoshimura[1, 2], *Maki* Mizuta[1], *Yujiro* Ikeda[1, 3], and *Yoshie* Otake[1]

[1]RIKEN Center for Advanced Photonics, Neutron Beam Technology Team, Wako, Saitama, Japan
[2]Tokyo Institute of Technology, Meguro, Tokyo, Japan
[3]J-PARC Center, Japan Atomic Energy Agency, Tokai, Ibaraki, Japan

Abstract. To meet strong demand for realizing an effective tool to diagnose salt distribution in concrete infrastructures, we have started a development of a new technique using a prompt gamma neutron activation analysis (PGNAA) at the RIKEN accelerator-driven compact neutron source (RANS). So far, by applying PGNAA we have experimentally confirmed that neutrons from RANS can detect small enough amounts of chlorine within the marginal concentration of around 1.2 kg/m^3 to involve steel corrosion. In this study, we have proposed two methods to derive the salt depth profile which is critical information of steel corrosion start. The first one utilizes a difference in the intensity ratio of two different γ-ray energies of interest, which is depending on the depth where the neutron capture reaction arises inside the concrete. The second is called the collimator method that measure γ-rays coming through a collimator around detector. Detection of γ-ray associated with ^{35}Cl coming from the assembly of concrete has been also simulated with conditions of neutrons from RANS and a collimator. The feasibility of the method was discussed.

1 Introduction

Concrete infrastructures like a bridge are suffered from chloride attack due to sea wind close to coast and anti-icing agent in mountain area both contain chloride. Chloride ions go into concrete structure and reach to near steel bar. Steel corrosion start from the chloride ion concentration in the range of 1.2 to 2.5 kg/m^3 [1], which is called the marginal concentration. As chloride attack progresses, decrease of steel cross section, crack of concrete, rust juice, and so on occur. But when these sign like a rust juice appear, chloride attack is already quit processing. Eventually, serious accident like a collapse of a bridge happen. Therefore, it is important to investigate the chloride ion concentration in concrete structures. Along with chloride ion concentration, to know its distribution between object surface and steel bar in concrete structure is especially important. Hereafter the distribution of chloride ion concentration is called “salt distribution”.

Several conventional methods for salt distribution measurement exist [2-4]. They need several steps before measurement. First step is core sampling from structure. Core is moved to experimental room. Then, pre-processing like a cutting, smashing, chemical treatment is applied. After measurement, mortar must be buried into hole after core sampling. In recently, handy device of X-ray fluorescence analysis exist without these steps. But it measures only surface, therefore it finally need core sampling to measure salt distribution. These methods are reliable and accurate, but there are disadvantages such as the limit of sampling location, taking long time, cost, and so on. For these reason, it is difficult to analyze many structures. Non-destructive technique without core sampling is desirable to assay many structures. To meet the demand, we have started the development of on-site non-destructive technique for salt distribution in concrete by prompt gamma neutron activation analysis (PGNAA) at the RIKEN accelerator-driven compact neutron source (RANS) [5]. So far, we have experimentally confirmed that RANS provides suitable neutron fluxes to detect small enough amounts of chlorine within the marginal concentration of around 1.2 kg/m^3 to involve steel corrosion, by applying PGNAA to 4x4x4cm^3 mortar bricks of different chloride ion concentrations from 0.36 to 5.1 kg/m^3 [6, 7].

In this work, we have proposed two methods to measure salt distribution. The first one utilizes a difference in the intensity ratio of two different γ-ray energies of interest, which is depending on the depth where the neutron capture reaction arises inside the concrete. Second one used γ-ray collimator. By collimating γ-ray detection area and neutron beam, γ-ray from target depth are detected. We call it collimator method. Then we carried out trial experiment to show the principle of these methods at RANS [8]. To confirm the feasibility of the concept of the proposed methods, we have performed the simulation with the Monte Carlo simulation code GEANT4 [9] for the production of γ-rays involved the neutron capture reaction of ^{35}Cl in the

* Corresponding author: y.wakabayashi@riken.jp

concrete assembly. The γ-rays were produced by injecting a collimated neutron beam into a concrete distributed salt uniformly and detected at concrete surface.

In this paper, we will introduce the feasibility of the proposed methods from the result of trial experiment and simulation.

2 Experiment for proposed methods

Experiment was performed at RANS shown in Figure 1. Neutrons are produced by using the reaction of 7MeV proton whose beam current is 100 ∝A at maximum with a beryllium target of 300∝m thickness. Neutron beam are extracted from a neutron guide, which we call N0, after the target station. N0 have an exit of 160x160 mm^2. By inserting an additional polyethylene collimator from this exit, neutron beam size can be adjusted.

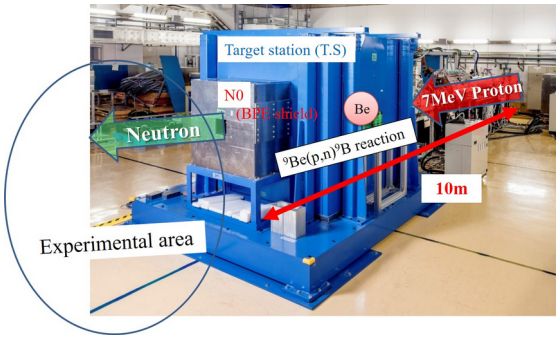

Figure 1 : Picture of RANS and experimental hall

2.1. Experimental Setup

Figure 2 shows the figure of experimental setups. The 30x30 cm^2 concrete bricks with 6-cm or 10-cm thickness were used. A salt sample was placed between concrete bricks and at different depth position from No.1 to No.3. To shield undesirable γ-rays and neutrons derived from RANS, lead bricks and LiF tiles were placed around detectors, concretes, and N0. A neutron collimator made of polyethylene with a hole of φ30mm was inserted into N0. For γ-ray collimators, lead bricks were placed with a gap of 2 cm. Salt of 250 g weight was put in paper box of 8 × 6 × 6 cm^3. Two Ge detectors were placed to view different depth position. In setup (I), they viewed No.1 and No.2 positions. After measurement at setup (I), right side detector was changed to view No.3 position as setup (II). Under these conditions, the γ-ray measurement was done.

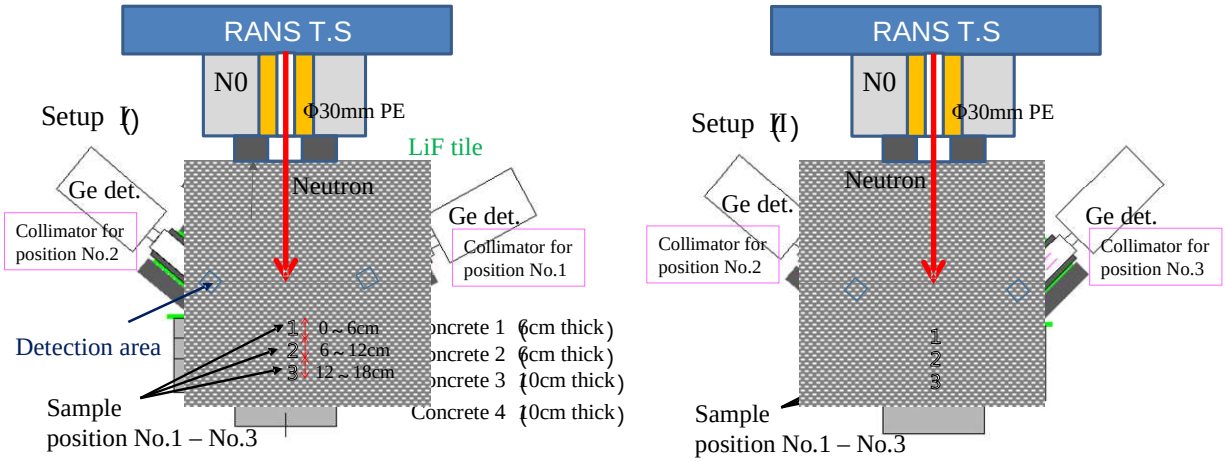

Figure 2 : Schematic views of experimental setups.

2.2 Gamma-ray spectra and γ-ray intensity ratio

Figure 3 shows the salt γ-ray spectra at sample positions of No1, No2, and No3 for the measuring time of 5, 10, and 20 minutes, respectively. The γ-rays derived from the ^{35}Cl(n,γ)^{36}Cl reaction, which are called as ^{35}Cl-γ-rays hereafter, are shown by arrows and appeared in spectra at all positions. This means that the γ-rays can be detected at concrete surface if salt exists within 12 cm depth in principle. Here, to deduce the depth of salt, the γ-ray intensity ratio method is explained. The γ-ray transmission T_γ in concrete is given as,

$$T_\gamma = exp(-d \times f_\gamma), \quad (1)$$

where d is a pass length of γ-ray in concrete, and f_γ is a γ-ray attenuation factor as shown in Table 1. The attenuation factors were obtained by using the database of NIST [10], weight ratios of a standard concrete composition shown in Table 2, and a density of 2.2 g/cm^3. Since transmissions in concrete for different γ-ray energies γ1 and γ2 are different, the ratio of transmissions has a relationship with a γ-ray intensity ratio of $I_{\gamma 1}/I_{\gamma 2}$ as shown below:

$$T_{\gamma 1}/T_{\gamma 2} = (A_{\gamma 1}/A_{\gamma 2}) \times (\varepsilon_{\gamma 2}/\varepsilon_{\gamma 1}) \times (I_{\gamma 2}/I_{\gamma 1}), \quad (2)$$

where $T_{\gamma 1}$ and $T_{\gamma 2}$ are transmission which can be calculated, $A_{\gamma 1}$ and $A_{\gamma 2}$ are the peak areas in γ-ray spectra, $\varepsilon_{\gamma 1}$ and $\varepsilon_{\gamma 2}$ are absolute γ-ray detection efficiencies measured with nothing between a standard γ-ray source and a γ-ray detector, $I_{\gamma 1}$ and $I_{\gamma 2}$ are the known relative intensity ratios [11]. In this work, 517, 788, 1165 keV as γ1 and 1951 keV as γ2 were used. The relative intensity ratios of several major ^{35}Cl-γ-rays are shown in Table 1.

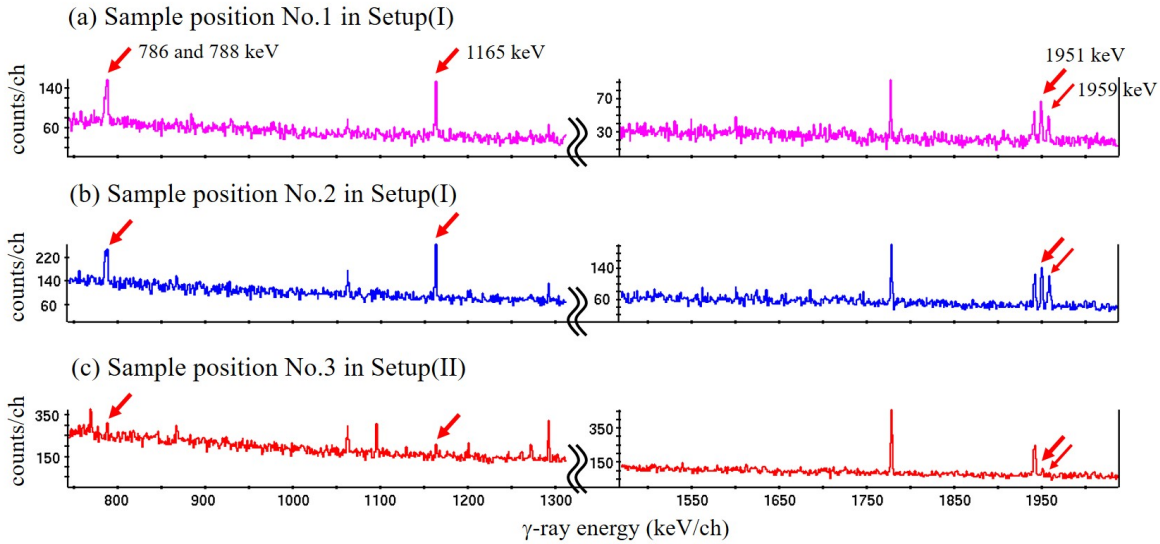

Figure 3 : Measured γ-ray spectra corresponding to sample positions.
(a) sample position No.1 in Setup(I), (b) sample position No.2 in Setup (I), and (c) sample position No.3 in Setup (II).
Arrows are γ-rays from ^{35}Cl(n,γ) reaction. The 786 and 788 keV γ-rays can't be separated clearly on this spectrum.

2.3 Validation of γ-ray intensity ratio and γ-ray collimator method

We performed the estimation of depth profile by using collimator method and γ-ray intensity ratio as shown in Figure 4 (a). Vertical axis is γ-ray intensity ratio based on the 1951 keV as reference γ-ray, and horizontal axis is γ-ray energy. Solid triangle, circle, and rectangle points in Figure 4 are experimental γ-ray intensity ratios at sample position No.1, No.2, and No.3, respectively, obtained from the right side of equation (2). These points are also plotted with error bars associated with peak fitting which include statistics errors. Solid, dashed, and dotted lines are γ-ray intensity ratios derived from calculations using equation (1) and the left side of equation (2).

In this experiment, salt sample has a thickness of 6 cm and the γ-ray collimators have the gap of 2 cm. Therefore, Ge detectors detect the γ-rays from different pass lengths in concrete like "Distance up" and "Distance down" as shown in Figure 4 (b). Then, we show two calculation lines of "Distance up" and

Table 1 : Major γ-energies, relative intensity ratios, and attenuation factors in capture reaction ^{35}Cl(n,γ)^{36}Cl

Eγ [keV]	Relative intensity ratio [%]	Attenuation factor [cm^{-1}]
517	85.07	0.191
786	38.37	0.158
788	60.83	0.158
1165	100	0.131
1951	71.04	0.100
1959	46.02	0.100
6111	73.96	0.058

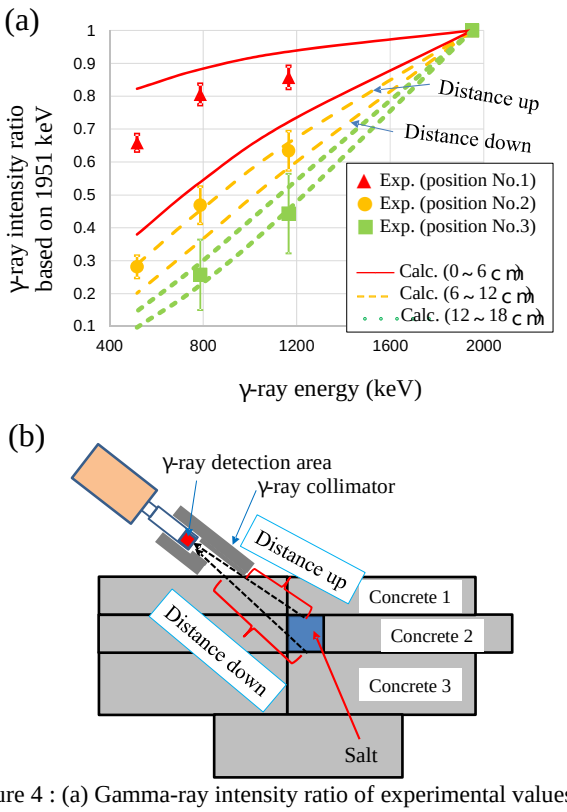

Figure 4 : (a) Gamma-ray intensity ratio of experimental values and calculation based on the 1951 keV γ-ray.
(b) Distance passing through concrete in case of position No.2.

Table 2. Weight ratios of elements contained in a standard concrete and the capture cross sections of thermal neutron of 25 meV.

Element	H	C	O	Mg	Al	Si	K	Ca	Fe	Cl
Cross section for thermal neutron (barn)	0.332	0.00386	0.00019	0.0630	0.230	0.165	2.058	0.429	2.565	33.15
Mix proportion (wt%)	1.03	0.1	54.46	0.22	3.48	34.6	0.22	4.46	1.43	---

"Distance down" for each sample position. From these experimental conditions, experimental values include uncertainties of the sample volumes and the pass lengths, and they are anticipated to be between two lines at each sample position.

Measured γ-ray intensity ratios are in between calculated lines for each sample position. It is indicated that the γ-ray collimator works well to detect γ-rays from each sample position and γ-ray intensity ratios are consistent with pass lengths in concrete for each sample position. Thus, we could conclude that the γ-ray intensity ratio method is consistent with the collimator method, and both are valid for depth profile measurement.

To confirm the experimental feasibility, further experimental with large area concrete of 30x30cm^2 including salt will be performed.

3 Simulation for the proposed methods

To confirm the feasibility of the proposed methods, simulation with GEANT4 [9] for the production of ^{35}Cl-γ-rays in the assembly was performed. In this simulation, from the point of view to detect ^{35}Cl-γ-rays effectively in a certain region at a depth of interest, we identified the optimum angle of the γ-ray collimator and then tried to find a way to estimate chloride ion concentration.

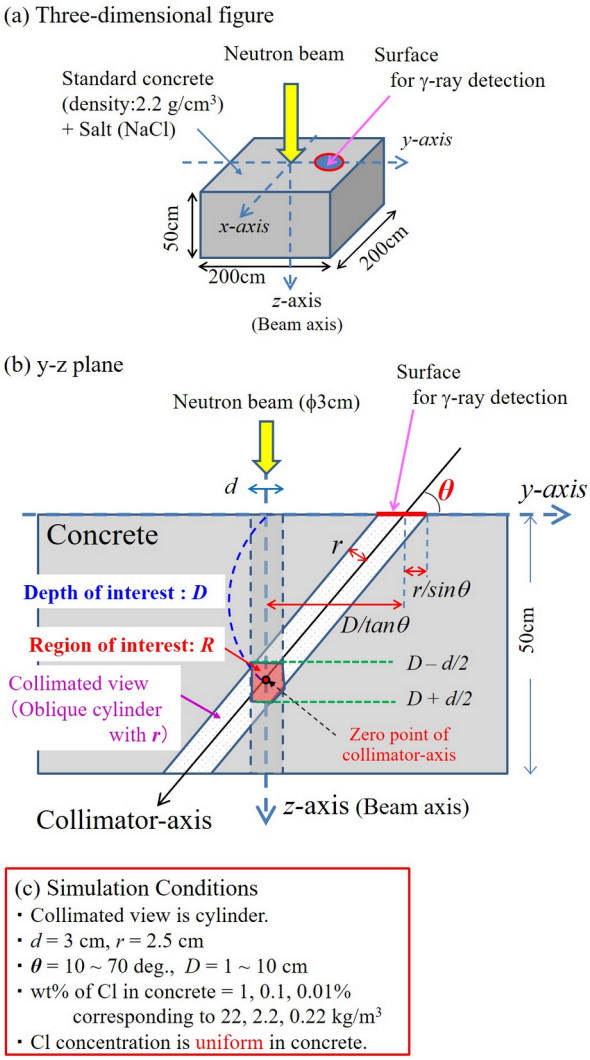

Figure 5 : Simulation geometries and conditions.
(a) Three-dimentional figure of geometries and coordinate.
(b) yz plane. (c) Summary of simulation conditions.

3.1. Simulation conditions

The simulation geometries and conditions of salt containing concrete are shown in Figure 5 (a)-(c), and are explained below. A 200 × 200 × 50 cm^3 standard concrete with salt was used. The compositions in concrete were same as ones shown in Table 2. Salt was homogeneously distributed in the concrete.

We defined that z-axis was the direction of neutron beam axis and x- and y-axes were directions along the concrete surface as shown in Figure 5 (a). In addition, we defined "collimator-axis" which had an angle θ with y-axis, and intersected z-axis as shown in Figure 5 (b). The zero point of this axis was a point across the z-axis. Neutron beam with a diameter of 3 cm and the energy spectrum of RANS [12] was injected to a concrete assembly.

The angle θ was defined as a collimator angle. As a view of a collimator looking into concrete, an oblique cylinder with radius *r* was defined, and called "collimated view" as shown in Figure 5 (b).

A depth of interest, where we aimed to measure the chloride ion concentration, was defined as *D*. A width to delimit a region in collimated view was defined as *d*, and was set to be 3 cm same as the diameter of neutron beam. Then, a region of interest "*R*" was defined as the region where z-axis and collimator-axis intersected and was delimited by *d* and *D*± *d/2* as shown in Figure 5 (b).

For the detection of ^{35}Cl-γ-rays produced in collimated view, we counted γ-rays passing through the surface with the area of $\pi(r/\sin\theta)^2$ as shown in Figure 5 (a) and (b). Here, it is noted that if we want to view different *D* at the same θ a distance between a center of surface for γ-ray detection and z-axis varies according to *D*/tan θ.

In this simulation, the amount in wt% of chlorine in concrete was changed from 0.01 to 0.1, and 1% corresponding to the chloride ion concentration of 0.22, 2.2, and 22 kg/m ^{3}, respectively. The collimator angle θ was changed from 10 to 70 degree. The depth of interest *D* was changed from 1 to 10 cm.

3.2 Production and detection rates of γ-rays

Figure 6 shows a contour plot of 35Cl counts in one of simulations as an example. This result was obtained by injecting neutrons of 1×10^9 under the conditions of Cl concentration of 2.2 kg/m^3, *D* = 10 cm, and θ = 30 degree. The unit of each point is counts. The region surrounded by dot ellipse is the production of ^{35}Cl-γ-rays in collimated view. The region of interest *R* is indicated by arrow and surrounded by rectangle.

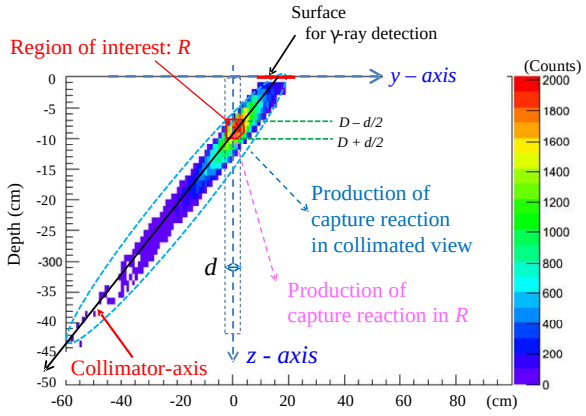

Figure 6 : Contour polt of ^{35}Cl production under simulation condisionts.

Here, the count of production is normalized to the production rate in unit of counts/s/100∝A, where 100 ∝A means the maximum proton beam current. Then, the production rate in collimated view and the production rate in *R* are plotted in collimator-axis as (a) and (b), respectively, in Figure 7. This production rate is a plot for the 1951 keV γ-ray under the conditions of Cl concentration of 22 kg/m^3, *D* = 5 cm, and θ= 30 degree.

Next, the production rate is converted to a detection rate that passes through the surface for γ-ray detection. A detection rate at a point in collimated view is calculated by following formula:

$$\textit{Detection rate} = (\textit{Production rate}) \times (\Omega/4\pi) \times T_\gamma, \quad (3)$$

where Ω is a solid angle and T_γ is a γ-ray transmission in concrete same as in Section 2. Then, the detection rate in collimated view and the detection rate in *R* become like (c) and (d), respectively, in Figure 7. As obvious, the detection rate along the axis increases as the position becomes close to the concrete surface although the production rate decreases. Positions between *R* and the surface dominate the detection of the γ-ray. On the other hand, the detection rate at a deeper region does not affect so much. Therefore, the key of our study is to identify the contribution of position closer to the surface with respect to that of *R*.

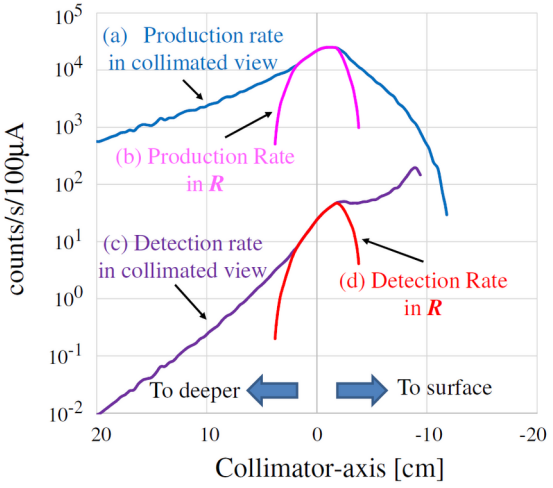

Figure 7 : Comparision with production rates and detection rates under the conditions of Cl concentration of 22 kg/m^3, *D* = 5 cm, and θ= 30 degree. (a) Production rate in collimated view. (b) Production rate in *R*. (c) Detection rate in collimated view. (d) Detection rate in *R*.

In following, to determine the optimum collimator angle, the detection rate was used for the estimation of Cl concentration.

3.3 Optimum collimator angle

To estimate optimum collimator angle, the ratio of the detection rates for the 1951 keV γ-ray in *R* and the total in collimated view were used. For effective detection of the ^{35}Cl-γ-rays in a region of interest, we assumed that an angle at which this ratio become highest should be optimum. Here, the detection rate in *R* is called *RR*, the total detection rate is called *TR*. The ratios of *RR* divide by *TR* are shown at the depths of interest *D* from 1 to 9 cm with θ= 10 to 70 degree in Figure 8. As a result, angles between 40 and 50 degree seem to be optimal for γ-ray detection in *R* at all depths as shown by the dashed rectangle in Figure 8. Although there is no clear indication, the θ= 50 seems preferable to θ= 40 at a low depth, and the 40 becomes effective at a deep depth.

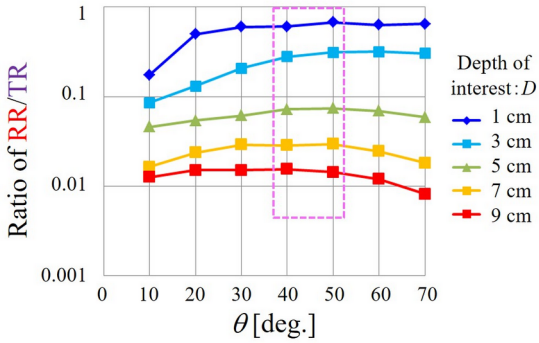

Figure 8 : Ratio of detection rate and total production rate at each depth of interest *D* for the 1951 keV γ-ray.

3.4 Estimation of chloride ion concentration

Figure 9 shows that RRs and TRs at the depths of interest *D* from 2.5 cm to 10 cm for the 1951 keV γ-ray for θ= 40 are plotted for chloride ion concentration of 0.22, 2.2, and 22 kg/m^3. It is shown that the ratios (*RR/TR*) are almost same for the different concentration at the same *D*. Assuming uniform chloride ion concentration in concrete, this result indicates that chloride ion concentration at *D* can be deduced from the ratios of *RR/TR* by obtaing *TR* experimentally. However, because the ratio is very small at depths larger than 7.5 cm, the estimation should have a large uncertainty. In addition to this uncertainty, we have to take into account uncertainties associated with the collimation. Because a collimated neutron beam brodens after coming out from

neutron collimator and a collimated view by using γ-ray collimator also brodens.

From the detection rate in this result, if a chloride ion concentration at *D* = 5cm is the merginal concentration [1] of 1.2 kg/m^3 which corresponds to 0.05 wt%, the *RR* is expected to be around 70 cps. Here, the γ-ray efficiency of the Ge detector with 10 % relative efficiency of 3"x3" NaI is about 0.05 % for the 1951 keV at 5-cm away from a γ-ray source. Then, the count rate of about 0.035 cps is expected at 5-cm away from the concrete surface, and the peak area becomes about 60 counts for about 30 minuetes. This count will be oberved in the γ-ray spectrum because the capture cross section [13] of chlorine is enough higher than other elements in the concrete composition as show in Table 2. In addtion, this measuring time is expected to be shorter than conventional methods. Therefore, it is expected that the proposed methods are feasible to estimate the chloride ion concentration at a depth up to 5 cm. Furthermore, although large unctertainties exist, the density at deeper region could be estimated.

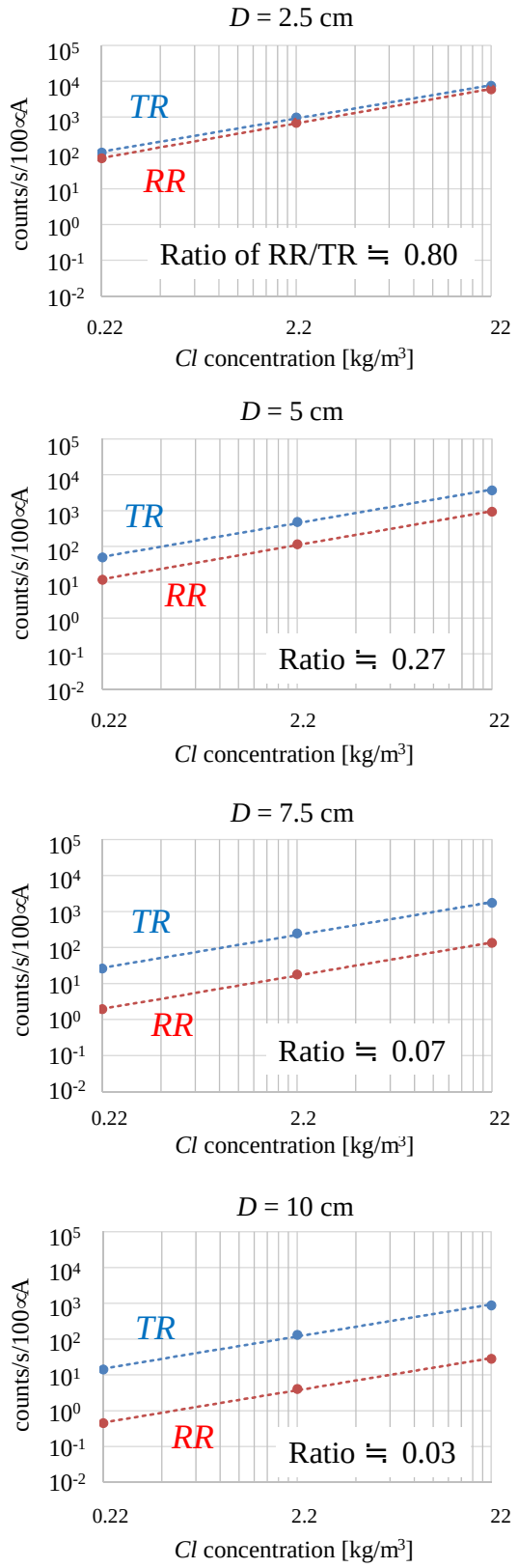

Figure 9 : Detection rate at the collimator angle of 40 degree for the 1951 keV γ-ray at each depth of interest *D* with chloride ion concentration of 0.22, 2.2, and 22 kg/m^3.

In the future, to evaluate and decrease the uncertainties, we will perfrom the simulation incorporating i) the broadening of a collimated neutron beam, ii) the broadening of a collimated view in concrete for γ-rays, and iii) the chloride ion concentration of non-uniform distribution in concrete. By validating the simulation, we will perform further experiments implementing an actual concrete structures.

4 Summary

Chlorine within 12 cm depth in concrete was detected by NPGA at RANS. The collimator method and the γ-ray intensity ratio seemed to be valid to measure salt distribution in concrete. It was shown that the optimum angle of γ-ray collimator was between 40 to 50 degrees, and the estimation of chloride ion concentration at a depth of interest up to 5 cm seemed to be possible using the ratio of *RR/TR* under assumption of the Cl uniform distribution.

This work was (partially) supported by Photon and Quantum Basic Research Coordinated Development Program from the Ministry of Education, Culture, Sport, Science and Technology, Japan, and Cross-ministerial Strategic Innovation Promotion Program (SIP), "Infrastructure maintenance, renovation and management" (Funding agency: JST).

References

1. JSCE, *Standard Specifications for Concrete Structures-2012 "Design"* (2012) (in Japanese)
2. JIS A 1154. *Methods of test for chloride ion content in hardened concrete* (in Japanese)
3. JSCE-G 574, Concrete Journal, **62**(1), 246 (2006) (in Japanese)
4. H. Kanada, Y. Ishikawa, and T. Uomoto, Concrete Journal, **44**(6), 16-23 (2006). (in Japanese)
5. Y. Otake, et al., J. Dis. Res. **12**(3), 585 (2017)
6. Y. Wakabayashi et al., *Proceedings of the Concrete Structure Scenarios*, JSMS, **17**, 659 (2017) (in Japanese)

7. Y. Wakabayashi et al., Plasma and Fusion Research, **13**, 2404052 (2018)
8. Y. Wakabayashi et al., *Proceedings of the Concrete Structure Scenarios*, JSMS, **18**, 635 (2018) (in Japanese)
9. J. Allison, K. Amako, J. Apostolakis et al., IEEE Transactions on Nuclear Science. **53**(1), 270 (2006)
10. National Institute of Standards and Technology, XCOM : Photon Cross Sections Database, https://physics.nist.gov/PhysRefData/Xcom/html/xcom1.html
11. National Nuclear Data Center, Thermal Neutron Capture γ's, https://www.nndc.bnl.gov/capgam/
12. Y. Wakabayashi et al., Journal of Nuclear Science Technology, **55**, 859 (2018)
13. K. Shibata, O. Iwamoto, T. Nakagawa, N. Iwamoto, A. Ichihara, S. Kunieda et al., Journal of Nuclear Science Technology, **48**(1), 1 (2011).